Darboux curves on surfaces II

Ronaldo Garcia, Rémi Langevin, Pawel Walczak

Darboux curves on surfaces II

Ronaldo Garcia*, Rémi Langevin and Paweł Walczak

Abstract. In 1872, Gaston Darboux defined a family of curves on surfaces in the 3-dimensional Euclidean space $\mathbb{E}^3$ which are preserved by the action of the Möbius group and share many properties with geodesics. Here, we study the Darboux curves from a dynamical viewpoint on special canal surfaces, quadrics and some Darboux cyclides. We also describe the generic behavior of Darboux curves near ridge points (zig-zag and beak-to-beak).

Keywords: Darboux curves, conformal geometry, space of spheres, canal surfaces, ridge points.

Mathematical subject classification: 53A30, 53C12, 53C50, 57R30.

1 Introduction

Geodesics on a surface are defined in terms of a Riemannian metric. Here we study a family of curves defined on a surface M contained in the 3-dimensional space $\mathbb{E}^3$ using only its conformal structure, called *Darboux curves*.

They are characterized by a relation between the geometry of the curve and of the surface: an osculating sphere to a Darboux curve is always tangent to the surface.

The study of these curves started with G. Darboux at end of 19^{th} century, and has been continued until now.

We adopt a dynamical viewpoint and focus on semi-local behavior near *ridge points* (see Subsection 2.3) and on global properties of these curves.

We first recall the construction of a flow, that we call *Darboux flow*, on the set $V(M)$ of spheres tangent to the surface M having a saddle contact at the tangency point associated to the Darboux curves. This construction and the correspondence between conformal properties of one parameter families of spheres

*Corresponding author.

tangent to a surface $M \subset \mathbb{S}^3$ or $M \subset \mathbb{E}^3$ along curves and properties of curves in $V(M)$ is the main topic of [11].

The unit tangent bundle T^1M is essentially a 4-fold covering of $V(M)$. There we can write a differential equation for a flow "covering" the Darboux flow (see Section 2.4 and [11]).

Then in Sections 4 and 5 we present a detailed study of the dynamical behavior of Darboux curves on special canal surfaces and quadrics, retrieving in particular results of [6], [7], [8], [15], [16], [25], [27], [29], [30], [31], [35].

The global study of Darboux curves in general remains wide open. In particular, it would be interesting to know on which surfaces there exist either closed and/or complete Darboux curves disjoint from the ridges.

2 Preliminaries

In this section we fix the notations and revise some results of [11].

2.1 Spheres tangent to a surface

In the Lorentz space $\mathbb{R}^5_1$ endowed with the Lorentz quadratic form $\mathcal{L} = -x_0^2 + x_1^2 + \cdots + x_4^2$, the points of the de Sitter quadric $\Lambda^4 \subset \mathbb{R}^5_1$ of equation $\mathcal{L} = 1$ represent oriented (plane-or-)spheres of $\mathbb{E}^3$ (see [17] and [21]). Through out the paper, except when explicitly mentioned, planes are considered as particular spheres.

We will use the terminology of relativity theory to qualify vectors of $\mathbb{R}^5_1$: v is space-like if $\mathcal{L}(v) > 0$, time-like if $\mathcal{L}(v) < 0$ and light-like if $\mathcal{L}(v) = 0$. A subspace will be space-like if it contains only space-like non-zero vectors, time-like if it contains some time-like non-zero vectors, and light-like if it contains some light-like non-zero vectors but no time-like non-zero vectors.

The points of $\mathbb{E}^3$ are represented by the intersection $\mathcal{E}$ of the light cone $\mathcal{L}ight$ given by equation $\mathcal{L} = 0$ and an affine hyperplane Q parallel to a hyperplane q tangent to $\mathcal{L}ight$. Such an hyperplane is tangent to $\mathcal{L}ight$ along a line of the form $\mathbb{R} \cdot m_\infty$. Therefore $q = m_\infty^\perp$. Any 3-dimensional subspace $\mathbb{E}$ of Q transverse to the direction m_∞ is space-like, therefore the restriction of $\mathcal{L}$ to it is positive definite. The restrictions of $\mathcal{L}$ to the tangent spaces at points of the paraboloid $\mathcal{E}$ form a Riemannian metric on $\mathcal{E}$. The Riemannian metric induced by $\mathcal{L}$ on $\mathbb{E}$ is Euclidean; the projection of $\mathcal{E}$ on $\mathbb{E}$ parallely to m_∞ is an isometry. This shows that the induced metric on $\mathcal{E}$ is also Euclidean. Alternatively, we may think of the set of generatrices of the light cone $\mathcal{L}ight$ as the completion $\mathbb{S}^3$ of $\mathbb{E}^3$.

Each time-like hyperplane h intersects $\mathcal{I}$ in a subset isometric to a sphere or a plane (see [17]). The space-like line $h^{\perp}$ intersects the quadric $\Lambda^4 = \{\mathcal{L} = 1\}$ at two points. Reciprocally, each point of Λ^4 corresponds to a sphere (or plane) endowed with an orientation.

If two points σ_1 and σ_2 of Λ^4 satisfy $\mathcal{L}(\sigma_1, \sigma_2) = 0$, the corresponding spheres (or planes) are orthogonal. If they satisfy $\mathcal{L}(\sigma_1, \sigma_2) = 1$, the corresponding spheres (or planes) are tangent (or parallel if both are planes). The set $T_\sigma \Lambda^4 \cap \Lambda^4$ is a cone of vertex σ which is a union of light-rays. A glance at Equation 1 below will convince the reader that each generatrix of this cone corresponds to spheres tangent to the sphere Σ associated to $\sigma \in \Lambda^4$ at a point $m \in \Sigma$.

The spheres tangent to a surface $M \subset \mathbb{E}^3$ form a 3-dimensional subset of the set of spheres, which is 4-dimensional (see [19]).

Let $V(M) \subset \Lambda^4$ be the set of spheres having a saddle contact with the surface $M \subset \mathbb{E}^3$.

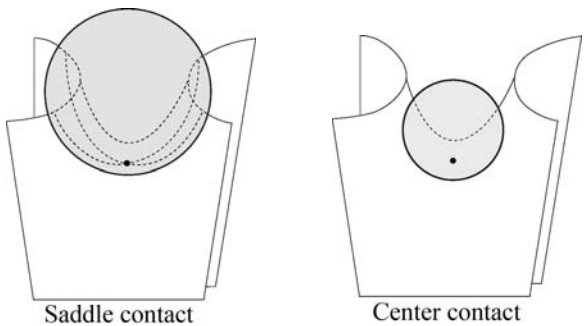

Figure 1: Possible contacts of a sphere and a surface.

The set $V(M)$ essentially projects on M. Indeed, generically, a point $\sigma \in V(M)$ projects on the tangency point of the sphere Σ corresponding to σ and the surface M (exceptional points of $V(M)$ correspond to spheres tangent to M at more than a point). Above any non umbilical point $m \in M$, the spheres admitting a saddle contact with M form a light-like segment bounded by the two osculating spheres at $m \in M$ (see [21] and [11]).

We will denote by $\mathcal{O}_1$ and $\mathcal{O}_2$ the surfaces of osculating spheres associated respectively to the principal curvatures $k_1 \geq k_2$ of the surface M and by $\mathcal{M}$ the surface of spheres tangent to M of mean curvature equal to the mean curvature of M at the tangency point.

The boundary of $V(M) \subset \Lambda^4$ is the surface $\mathcal{O}_1 \cup \mathcal{O}_2$ of spheres osculating M. Therefore, when M has no umbilics, $V(M)$ is essentially an interval fiber-bundle $\pi : V(M) \to M$ over M. The fibers I_m are light-like intervals.

The points σ_α of a fiber I_m can be expressed as linear combinations of the two osculating spheres $o_1(m)$ and $o_2(m)$: $\sigma_\alpha = \cos^2\alpha\, o_1(m) + \sin^2\alpha\, o_2(m)$.

Euler's computation of the normal curvatures $k_n = k_n(m, \ell)$ of sections of a surface by normal planes intersecting the tangent plane T_mM along a line ℓ making angle α with the first principal direction implies

Proposition 1. *Let $k_n = k_1\cos^2\alpha + k_2\sin^2\alpha$. Then the angle of the two directions $\ell_{\pm\alpha}$ tangent at m to $\Sigma_{m,k_n} \cap M$ with the principal direction corresponding to k_1 is $\pm\alpha$, where Σ_{m,k_n} is the sphere tangent to M at m of curvature k_n, that is such that geodesic circles on Σ_{m,k_n} have curvature k_n.*

Proof. See [11]. □

The interval bundle $V(M)$ is closely related with the projective tangent bundle $\mathbb{P}(T(M))$. Indeed, let us chose as origin on a fiber of $\mathbb{P}(T(M))$ the direction of the first principal direction. The "antipodal" direction of the first principal direction on the fiber P_m of $\mathbb{P}(T(M))$ above m is the second principal direction. Sending the direction making an angle α with the first principal direction and the one making an angle $-\alpha$ to the point $\sigma_\alpha \in I_m$ "folds" the circle P_m on the interval I_m.

When M has umbilical points, the two folds $\mathcal{O}_1$ and $\mathcal{O}_2$ meet at the osculating spheres at umbilical points of M. The middle-points of the segments $[o_1(m), o_2(m)], m \in M$ form a surface $\mathcal{M}$, the *mean surface*. Each point of $\mathcal{M}$ is a sphere tangent to M at a point m. Moreover its mean curvature is equal to the mean curvature $\mathcal{H}(m)$ of M at m. R. Bryant noticed that the area of this surface is the value of the Willmore functional for M (see [4]).

It is convenient to have a formula giving the point $\sigma \in \Lambda^4$ in terms of the Riemannian geometry of the corresponding sphere $\Sigma \subset \mathcal{E} \subset \mathcal{L}ight$ and a point m on it. For that we need to know also the unit vector $\vec{n}$ tangent to $\mathcal{E} \subset \mathcal{L}ight$ and normal to Σ at m and the geodesic curvature k of Σ, that is, for us, the geodesic curvature (as a curve of $\mathcal{E} \subset Q \subset \mathbb{R}^5_1$) of any great circle on Σ. We can also think of k as the curvature of any great circle on $\Sigma \subset \mathcal{E}$, where $\mathcal{E}$ is endowed with its Euclidean metric induced from $\mathcal{L}$.

Proposition 2. *The point $\sigma \in \Lambda^4$ corresponding to the sphere $\Sigma \subset \mathcal{E} \subset \mathcal{L}ight$ is given by*

$$\sigma = k \cdot m + \vec{n}. \tag{1}$$

Proof. See for example [17] Section 1.1 and [20]. □

2.2 Local conformal invariants of surfaces

Assume that M is a surface which is *umbilic free*, that is, that the principal curvatures $k_1(x) \geq k_2(x)$ of M are different at any point x of M. We will keep the convention $k_1 \geq k_2$ throughout the paper and refer to the principal direction associated to k_1 as *first* principal direction. Let X_1 and X_2 be unit vector fields tangent to the curvature lines corresponding to, respectively, k_1 and k_2. Put $\mu = (k_1 - k_2)/2$. Since more than 100 years, it is known ([34], see also [5]) that the vector fields $\xi_i = X_i/\mu$ and the coefficients θ_i $(i = 1, 2)$ in

$$[\xi_1, \xi_2] = -\frac{1}{2}(\theta_2\xi_1 + \theta_1\xi_2) \tag{2}$$

are invariant under arbitrary (orientation preserving) conformal transformation of $\mathbb{R}^3$. In fact, they are invariant under arbitrary conformal change of the Riemannian metric on the ambient space. This follows form the known (see [21], page 142, for instance) relation $\tilde{A} = e^{-\phi}(A - g(\nabla\phi, N) \times \mathrm{Id})$ between the Weingarten operators of a surface M with respect to conformally equivalent Riemannian metrics $\tilde{g} = e^{2\phi}g$ on the ambient space; here $\nabla\phi$ and N denote, respectively, the g-gradient of ϕ and the g-unit normal to M. Elementary calculation involving Codazzi equations shows that

$$\theta_1 = \frac{1}{\mu^2} \cdot X_1(k_1) \quad \text{and} \quad \theta_2 = \frac{1}{\mu^2} \cdot X_2(k_2). \tag{3}$$

The quantities θ_i $(i = 1, 2)$ are called *conformal principal curvatures* of M.

Let ω_1, ω_2 be the 1-forms dual to the vectors ξ_1, ξ_2. Then the equalities

$$d\omega_1 = \frac{1}{2}\theta_2\omega_1 \wedge \omega_2, \quad d\omega_2 = \frac{1}{2}\theta_1\omega_1 \wedge \omega_2 \tag{4}$$

hold. See [11].

2.3 Ridges

Let $\mathcal{F}_0$ and $\mathcal{F}_{\frac{\pi}{2}}$ be the foliations of M by lines of principal curvature associated respectively to the principal curvatures $k_1 \geq k_2$; these foliations are singular if M has umbilical points. For the generic behavior of $\mathcal{F}_0$ and $\mathcal{F}_{\frac{\pi}{2}}$ near umbilical points see [13] and references therein. Consider a surface M and a principal chart (u, v) such that the horizontal foliation $\mathcal{F}_0$ is that associated to the principal curvature k_1.

Definition 3. A non umbilical point $p_0 = (u_0, v_0)$ is called a *ridge point* of the principal foliation $\mathcal{F}_0$ if $\frac{\partial k_1}{\partial u}(p_0) = 0$, equivalently, if $\theta_1(p_0) = 0$. In the same way we define ridges for $\mathcal{F}_{\frac{\pi}{2}}$.

We refer the reader to [26] for an introduction to ridges and to [14] for application to the construction of eye-lenses.

Let us pull back the foliation $\mathcal{F}_0$ of M to a foliation $\tilde{\mathcal{F}}_0$ of $\mathcal{O}_1$. The lift of a ridge point to $\mathcal{O}_1$ is in general a cusp of a leaf L of $\tilde{\mathcal{F}}_0$. To see that, let us parametrize a leaf L of $\mathcal{F}_0$ near a ridge point using a regular parameter t on the corresponding line of curvature. It induces a parametrization of the corresponding leaf $\tilde{L} = \{o_1 = o_1(t)\}$ of $\tilde{\mathcal{F}}_0$. Then, at a ridge point, $k_1' = 0$. Differentiating (1) we get, at the lift of the ridge point, $o_1' = 0$.

The correspondence between singular points of $\mathcal{O}_i$ and ridges can be seen directly observing that the osculating spheres along their line of principal curvature are stationary at a ridge point. From that it follows that ridges are conformally defined.

In general, ridge points form curves in M that we call just *ridges*. The lift to $\mathcal{O}_1$ of a ridge for k_1 is in general a cuspidal edge of the surface $\mathcal{O}_1$. See Figure 2.

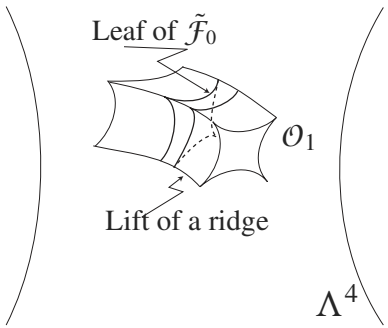

Figure 2: The surface $\mathcal{O}_1$ and the foliation $\tilde{\mathcal{F}}_0$.

The equations of the two families of ridges are $\theta_1 = 0$ and $\theta_2 = 0$; let us define $\zeta_1 = \xi_1(\theta_1)(p_0)$ and $\zeta_2 = \xi_2(\theta_2)(p_0)$. In [11] we proved the following

Theorem 4. *Let p_0 be a point of a ridge of M corresponding to the principal foliation $\mathcal{F}_0$ such that $\zeta_1(p_0) \neq 0$. Then the ridge R containing p_0 is locally a regular curve transverse to $\mathcal{F}_0$; the boundary component of $V(M)$ corresponding to $\alpha = 0$ has a cuspidal edge along $\pi^{-1}(R)$, see Figure 3. The same is true for ridges associated to the principal foliation $\mathcal{F}_{\frac{\pi}{2}}$.*

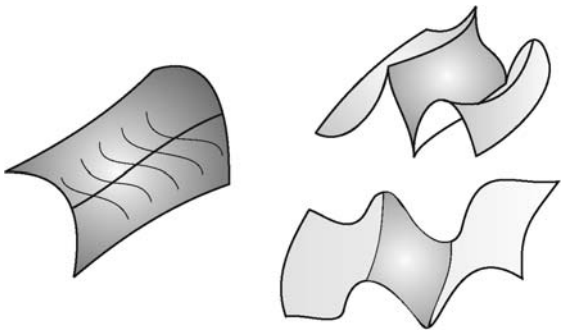

Figure 3: Ridges and Singularities of the boundary of $V(M)$.

For an open and dense set of compact surfaces with the C^r-topology of Whitney, $r \geq 4$, the set of ridge points is the union of regular curves outside the set of umbilical points. See [3].

Proposition 5. *At regular points, $V(M)$ inherits from Λ^4 a semi-Riemannian metric. In other words its tangent 3-space at any regular point is light-like.*

2.4 Differential equation of a Darboux curve in a principal chart

Definition 6. A curve C on a surface $M \subset \mathbb{E}^3$ is a *Darboux curve* if at each point $m \in C \subset M$ the osculating sphere to C at m is tangent to M at m.

We observe that the definition of Darboux curves involves only spheres and contact order, so this notion belongs to conformal geometry.

We prove in [11] the following

Theorem 7. *A curve $C \subset M$ is a Darboux curve if and only if it satisfies the equation*

$$k_n' + \tau_g k_g = 0, \tag{5}$$

where we differentiate with respect to the arc-length of C. Here k_n is the normal curvature, τ_g is the geodesic torsion and k_g is the geodesic curvature of $C \subset M$.

We also explain there that the osculating spheres to a Darboux curve form a curve which is a geodesic of the 3-dimensional space $V(M)$ of spheres having a saddle contact with the surface M. These curves, that we call $\tilde{D}$-curves form almost a flow: two such curves pass through every point of the interior of $V(M)$. To get a flow, we should "unfold" the intervals of light-ray fibering $V(M)$ into circles, that is consider the map $\mathbb{P}(TM) \to V(M)$, $(\alpha \bmod \pi \mapsto \sigma_\alpha$ (see Section 2.1)).

In fact we will consider, in order to compute using an angle $\alpha \in \mathbb{S}^1$, the unit tangent bundle T^1M of M, double cover of $\mathbb{P}(TM)$. T^1M covers four times the set of regular points of $V(M)$, and is endowed with a flow the orbits of which project onto $\tilde{D}$-curves.

Consider a local principal chart (u, v) in a surface $M \subset \mathbb{E}^3$.

We denote by s the arc-length of a curve C and by s_c, *mean-spheres length*, the arc-length of the curve corresponding to C in the surface $\mathcal{M}$ of mean spheres tangent to M. Length elements ds_c and ds are related by $\frac{ds_c}{ds} = \mu = \frac{(k_1-k_2)}{2}$.

Theorem 8. *Let (u, v) be a principal chart and $C : s \mapsto c(s)$ a Darboux curve parametrized by Euclidean arc length s or mean-sphere length s_c. Let α be the angle between C and the principal direction $\partial/\partial u$. The angle α satisfies the following differential equation*

$$6 \sin\alpha \cos\alpha \, \frac{d\alpha}{ds_c} = \theta_1 \cos^3\alpha + \theta_2 \sin^3\alpha. \tag{6}$$

Notice that all the quantities involved in Equation (6) are conformally defined. Equation (6) implies directly that the Darboux curves on a Dupin cyclide ($\theta_1 = \theta_2 = 0$) make a constant angle with the principal curvature lines. The Darboux curves are then exactly the leaves of the foliations $\mathcal{F}_\alpha$ studied in [12].

2.5 A plane-field on $V(M)$

In this subsection we consider a natural plane-field associated to the Darboux curves and its integrability in terms of conformal invariants.

Two tangent vectors $\mathcal{D}_1$ and $\mathcal{D}_2$ to the two Darboux curves through the point $(m, \alpha) \in V(M)$ define a plane in $T_{m,\alpha}V(M)$. These planes define a plane-field $\mathcal{D}$. It will be called *Darboux plane-field*. As a branch of the intersection of a sphere $\sigma_{m,\alpha}$ and M, and the Darboux curve tangent at m to this branch have the same osculating circle, the vector, say $\mathcal{D}_1$, is also tangent to the pencils of spheres through this osculating circle. The plane $\mathcal{D}$ is therefore tangent at $(m, \alpha) \in V(M)$ to the two curves corresponding to pencils through the osculating circles to the two branches.

The next results, see [11], establish the necessary and sufficient conditions of integrability of the Darboux plane-field $\mathcal{D}$.

Theorem 9. *The Darboux plane-field $\mathcal{D}$ is integrable if and only if*

$$\xi_1(\theta_2) = -\frac{5}{6}\theta_1\theta_2, \qquad \xi_2(\theta_1) = \frac{5}{6}\theta_1\theta_2. \tag{7}$$

Corollary 10. *Consider a principal chart (u, v) and principal curvatures $k_1 > k_2$. Then the criterium of integrability of the Darboux plane-field $\mathcal{D}$ is given by:*

$$\begin{aligned}\frac{\partial^2 k_1}{\partial u \partial v} &= \frac{1}{3} \cdot \frac{1}{k_1 - k_2} \frac{\partial k_1}{\partial u} \left(3\frac{\partial k_1}{\partial v} - \frac{\partial k_2}{\partial v} \right) \\ \frac{\partial^2 k_2}{\partial u \partial v} &= \frac{1}{3} \cdot \frac{1}{k_1 - k_2} \frac{\partial k_2}{\partial v} \left(\frac{\partial k_1}{\partial u} - 3\frac{\partial k_2}{\partial u} \right)\end{aligned} \tag{8}$$

3 Local and semi-local dynamics of Darboux curves

In this section we study the local and semi-local aspects of Darboux curves near a non-ridge point and regular arcs of ridge points transversal to the associated principal foliation, called zig-zag and beak-to-beak. Then we determine the dynamical behavior of Darboux curves on non-degenerated quadrics near the ridges.

3.1 Darboux curves near non-ridge points and near arcs of ridges

In this subsection we consider the dynamical behavior of Darboux curves through a non-ridge point and near a regular arc of ridge points.

More precisely, we analyze the asymptotic behavior of Darboux curves when the curve becomes tangent to a principal direction and consider the qualitative behavior of Darboux curves near a regular ridge point where the ridge is transverse to the correspondent principal foliation. We analyze in this situation the generic behavior of the Darboux curves: there are two different patterns, zig-zag and beak-to-beak, see Figure 6.

Proposition 11. *Let p_0 be non-umbilical point which is not in a ridge, i.e. $\theta_i(p_0) \neq 0$, $(i = 1, 2)$, and consider a principal chart (u, v) that is a chart such that the coordinate curve $v = constant$ ("horizontals") are plaques of the foliation $\mathcal{F}_0$ associated to the principal curvature k_1, and the the coordinate curve $u = const.$ ("verticals") are plaques of the foliation $\mathcal{F}_{\frac{\pi}{2}}$ to the principal curvature k_2.*

The Darboux curves tangent to the lines of principal curvature at p_0 are singular curves of cuspidal type and are parameterized by

$$(u(t), v(t)) = \left(\frac{1}{24}(k_1 - k_2)\theta_1 t^2 + \cdots, \frac{1}{216}(k_1 - k_2)^2 \theta_1^2 t^3 + \cdots \right)$$

and

$$(u(t),\, v(t)) = \left(\frac{1}{216}(k_1 - k_2)^2\theta_2^2 t^3 + \cdots,\, \frac{1}{24}(k_1 - k_2)\theta_2 t^2 + \cdots\right).$$

The behavior of the Darboux curves passing through p_0 is as shown in Figure 4.

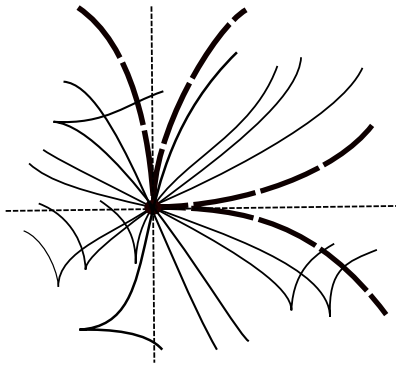

Figure 4: Darboux curves through a non-ridge point. The right side of the figure shows the cuspidal contact of the Darboux curves with the principal line (horizontal) and the top side the same behavior with the other principal line (vertical).

Proof. From the differential equation (6) it follows that the Darboux curves in M are the projections of the integral curves of the vector field $\mathcal{D}_1$ defined in the tangent bundle $TM \setminus \{v_1, v_2\} = \{(p, v) : v \in T_pM,\, v \neq v_1,\ v \neq v_2\}$, where $\{v_1, v_2\}$ is the set of principal directions. In a local chart (u, v, α) it is given by

$$\mathcal{D}_1 = \left[\frac{\cos\alpha}{\sqrt{E}}\frac{\partial}{\partial u} + \frac{\sin\alpha}{\sqrt{G}}\frac{\partial}{\partial v}\right]$$
$$+ \left[\frac{\partial k_1/\partial u}{3\sqrt{E}(k_1 - k_2)}\frac{\cos^2\alpha}{\sin\alpha} + \frac{\partial k_2/\partial v}{3\sqrt{G}(k_1 - k_2)}\frac{\sin^2\alpha}{\cos\alpha}\right]\frac{\partial}{\partial\alpha}.$$

To develop the analysis we will consider the vector field $X = \cos\alpha\sin\alpha\,\mathcal{D}_1$ defined by the differential equation:

$$u' = \frac{1}{\sqrt{E}}\cos^2\alpha\sin\alpha\,, \qquad v' = \frac{1}{\sqrt{G}}\sin^2\alpha\cos\alpha\,,$$
$$\alpha' = \frac{k_1 - k_2}{12}[\theta_1\cos^3\alpha + \theta_2\sin^3\alpha]\,.$$

The vector field X has a smooth extension to the axis α. Also, $X(u, v, \alpha+\pi) = -X(u, v, \alpha)$ and therefore it projects (as a line-field) smoothly to the projective bundle $P(TM)$.

For any initial condition $(0, 0, \alpha_0)$, with $\alpha_0 \neq \frac{n\pi}{2}$, $n \in \mathbb{Z}$, the integral curves of X are transverse to the axis α and therefore have regular projections. For $\alpha_0 = \frac{\pi n}{2}$ and $\theta_1\theta_2 \neq 0$, the integral curves of X have quadratic tangency with the axis α and under the hypothesis the projections of these integral curves are singular curves of cuspidal type, see Figure 5.

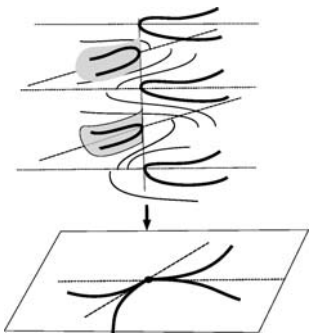

Figure 5: Projections of integral curves of X in the singular Darboux curves through a non-ridge point.

In fact, for $\alpha = n\pi$ and assuming the normalization $E(0) = G(0) = 1$, direct calculations provide

$$\begin{aligned} u(t) =& \frac{1}{24}(k_1 - k_2)\theta_1 t^2 + \cdots \\ v(t) =& (-1)^n \frac{1}{216}(k_1 - k_2)^2\theta_1^2 t^3 + \cdots \\ \alpha(t) =& n\pi + (-1)^n \frac{\theta_1}{12} t + \cdots \end{aligned}$$

For $\alpha = \frac{n\pi}{2}$ direct calculations provide

$$\begin{aligned} u(t) =& \frac{1}{216}(k_1 - k_2)^2\theta_2^2 t^3 + \cdots \\ v(t) =& (-1)^n \frac{1}{24}(k_1 - k_2)\theta_2 t^2 + \cdots \\ \alpha(t) =& \frac{n\pi}{2} + (-1)^{n-1} \frac{\theta_2}{12} t + \cdots \end{aligned}$$

Now observe that the projection $P(u, v, \alpha) = (u, v)$ of the integral curves of X passing through $(0, 0, n\pi)$ and $(0, 0, \frac{n\pi}{2})$ form a cusp tangent to a principal curvature line. □

Remark. We do not know if Darboux curves issued from a non-ridge point m cover a neighborhood of m deprived of the lines of principal curvature through m.

Recall, see Definition 3, that a non umbilical point $p_0 = (u_0, v_0)$ is called a *ridge* point of the principal foliation $\mathcal{F}_0$ or of the principal curvature k_1 if $\frac{\partial k_1}{\partial u}(p_0) = 0$, equivalently, if $\theta_1(p_0) = 0$. In the same way we define ridges for $\mathcal{F}_{\frac{\pi}{2}}$.

Recall that the ridge points are associated to the singularities of the focal set of the surface and also to the singularities of the boundary of $V(M)$ (see Section 2.1).

Definition 12. A ridge point p_0 of $\mathcal{F}_0$ is called *zig-zag*, when

$$\zeta_1(p_0) = \frac{\partial^2 k_1}{\partial u^2}(p_0) \Big/ (k_1(p_0) - k_2(p_0)) < 0,$$

or equivalently when $\xi_1(\theta_1)(p_0) < 0$.

It is called *beak-to-beak*, when $\zeta_1(p_0) > 0$, or equivalently when $\xi_1(\theta_1)(p_0) > 0$.

We define zig-zag and beak-to-beak points for $\mathcal{F}_{\frac{\pi}{2}}$ in the same way. In this case a point p_0 is a ridge *zig-zag* when $\xi_2(\theta_2)(p_0) < 0$ and it is beak-to-beak when $\xi_2(\theta_2)(p_0) > 0$.

Theorem 13. *Let R be an arc of ridge points transverse to the corresponding principal foliation (i.e., suppose that $\zeta_i(p) \neq 0$ for every $p \in R$). Then there exist exactly two types of behavior for the Darboux curves near the ridge arc R, zig-zag $\zeta_i(p) < 0$ and beak-to-beak $\zeta_i(p) > 0$ as shown in Figure 6.*

Proof. Consider the vector field X as in the proof of Proposition 11.

We will consider a ridge corresponding to $\mathcal{F}_0$. For the other principal foliation the analysis is similar.

The ridge is defined by the equation $\frac{\partial k_1}{\partial u}(u, v) = 0$.

In the principal chart (u, v), the singularities of the vector field X are given by $(R_1(v), 0) = (U(v), v, 0)$.

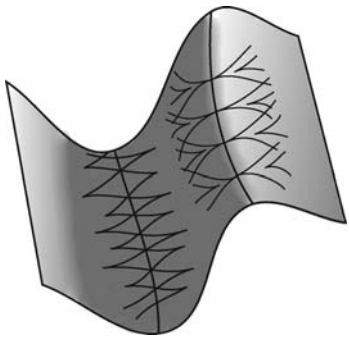

Figure 6: Darboux curves near regular arcs of ridges: zig-zag and beak-to-beak.

It follows that

$$DX(R_1(v),0)=\begin{pmatrix} 0 & 0 & 1\\ 0 & 0 & 0\\ \frac{1}{12}\frac{\partial\theta_1}{\partial u}(k_1-k_2) & \frac{1}{12}\frac{\partial\theta_1}{\partial v}(k_1-k_2) & 0\end{pmatrix}$$

The eigenvalues of $DX(R_1(v),0)$ are

$$\lambda_1=0,\quad \lambda_2=\frac{1}{2\sqrt{3}}\sqrt{\frac{\partial\theta_1}{\partial u}(k_1-k_2)},\quad \lambda_2=-\frac{1}{2\sqrt{3}}\sqrt{\frac{\partial\theta_1}{\partial u}(k_1-k_2)}.$$

Using invariant manifold theory, (see [18, page 44] and [9]), we see that when λ_2 and λ_3 are real and

$$\lambda_2\lambda_3=-\frac{1}{12}\frac{\partial\theta_1}{\partial u}(k_1-k_2)=-\frac{1}{3}\zeta_1(R_1(v))<0,$$

(hyperbolic case) the singular set of X (ridge) is normally hyperbolic. Therefore there exist stable and unstable surfaces, which are normally hyperbolic along the singular set. This implies that there is a lamination (continuous fibration) along the ridge and the fibers are the Darboux curves.

Darboux curves are as shown in Figure 6, right. That is, there are Darboux curves crossing the ridge, tangent to the lines of principal curvature, and these prolonged Darboux curves are C^1 along the ridge.

When

$$\zeta_1(R_1(v))=\frac{\partial^2 k_1}{\partial u^2}/(k_1-k_2)<0,$$

the non zeros eigenvalues of $DX(R_1(v),0)$ are purely complex (elliptic case) and therefore the singular set is not normally hyperbolic.

In this case we are in the hypothesis of Roussarie Theorem, [28, Theorem 20, page 59], so there is a local first integral in a neighborhood of the ridge. The level sets of this first integral are cylinders and the integral curves (like helices) in each cylinder when projected in the surface M have a cuspidal point exactly when the helix cross the section $\alpha = 0$. See Figure 7.

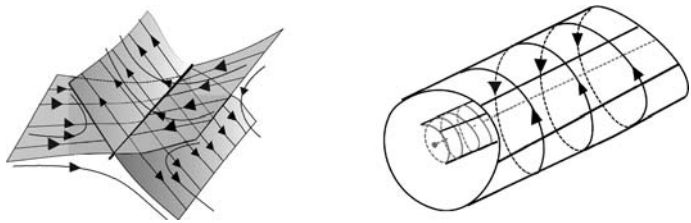

Figure 7: Integral curves of X near a curve of singularities: hyperbolic an elliptic behavior.

The projections of integral curves of X in M produces the zig-zag as shown in Figure 6, left.

There are no Darboux curves tangent to the principal direction $\partial/\partial u$ along the ridge in this case.

A similar analysis for the other ridge corresponding to principal foliation $\mathcal{F}_{\frac{\pi}{2}}$ can be carried out. □

3.2 Darboux curves near ridges on quadrics

In this subsection we describe the dynamical behavior of Darboux curves near the ridges on non-degenerated quadrics (ellipsoids and hyperboloids). The global study of Darboux curves on quadrics will be done in Section 5.

Proposition 14. *The ridges of* $\mathbb{Q}_{a,b,c} = \{(x, y, z) : x^2/a + y^2/b + z^2/c = 1\}$ *are the intersection of the quadric with the coordinates planes. Moreover the conic that contains the umbilical points is divided in connected components of the ridges of* k_1 *and* k_2. *See Figure 8.*

Proof. By the symmetry it is clear that the points of intersection of the coordinate planes with the quadric are ridges points. In a principal chart (u, v), see equation (12), we have that

$$\frac{\partial k_1}{\partial u} = -\frac{3}{2u}k_1 \neq 0 \quad \text{and} \quad \frac{\partial k_2}{\partial v} = -\frac{3}{2v}k_2 \neq 0.$$

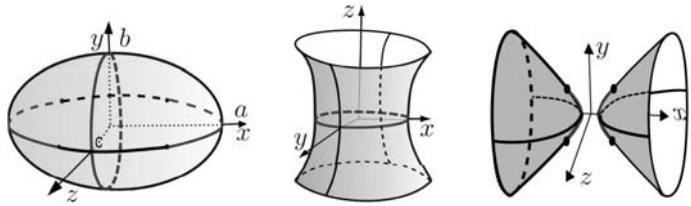

Figure 8: Ridges of the quadric $\mathbb{Q}_{a,b,c}$.

Therefore the principal curvatures have no critical points along the corresponding principal curvature line in the complement of these three conics. This implies that there are no ridges outside the intersection of the coordinate planes with the quadric. □

Proposition 15. *Consider the quadric*

$$\mathbb{Q}_{a,b,c} = \left\{(x, y, z) : x^2/a + y^2/b + z^2/c = 1\right\}$$

and fix an orientation on it such that $k_1 \geq k_2$.

a) *For the ellipsoid with* $0 < c < b < a$ *it follows that*

   i) *The ellipse* $E_{xz} = \{y = 0\} \cap \mathbb{Q}_{a,b,c}$ *containing the four umbilics* $(x_0, 0, z_0)$ *is the union of ridges of* k_1 *and* k_2. *For* $|x| > x_0$ *the ridge correspond to* k_1. *The ellipse* E_{xz} *is beak-to-beak in both cases.*

   ii) *The ellipse* $E_{xy} = \{z = 0\} \cap \mathbb{Q}_{a,b,c}$, *respectively* $E_{yz} = \{x = 0\} \cap \mathbb{Q}_{a,b,c}$, *is a ridge corresponding to* k_1, *respectively to* k_2, *and is zig-zag.*

b) *For the hyperboloid of one sheet with* $c < 0 < b < a$ *it follows that*

   i) *The hyperbole* $H_{yz} = \{x = 0\} \cap \mathbb{Q}_{a,b,c}$ *is a ridge corresponding to* k_1 *and is beak-to-beak.*

   ii) *The hyperbole* $H_{xz} = \{y = 0\} \cap \mathbb{Q}_{a,b,c}$ *is a ridge corresponding to* k_1 *and is zig-zag.*

   iii) *The ellipse* $E_{xy} = \{z = 0\} \cap \mathbb{Q}_{a,b,c}$ *is a ridge corresponding* k_2 *and it is zig-zag.*

c) *For the hyperboloid of two sheets with* $c < b < 0 < a$ *it follows that*

   i) *The hyperbole* H_{xz} *is a ridge corresponding to* k_1 *and is zig-zag.*

ii) *The hyperbole H_{xy} containing the four umbilics $(x_0, y_0, 0)$ is the union of ridges of k_1 and k_2. For $|x| > x_0$ the ridge correspond to k_1 and all segments of hyperbolas are beak-to-beak.*

Proof.

a) Ellipsoid

It will be sufficient to check the condition of zig-zag or beak-to-beak only at a point of a connected component of the ridge.

The ellipse E_{xz} contained in the plane $y = 0$ contains the four umbilics U_i $(i = 1, \ldots,)$ and therefore E_{xz} is the ridge of $\mathcal{F}_0$ and $\mathcal{F}_{\frac{\pi}{2}}$. More precisely, under the hypothesis $a > b > c$ the arcs of ellipse that contain the vertices $(\pm\sqrt{a}, 0, 0)$ are ridges of $\mathcal{F}_{\frac{\pi}{2}}$ and the arcs of ellipse that contain the vertices $(0, 0, \pm\sqrt{c})$ are ridges of $\mathcal{F}_0$.

Consider the point $p_0 = (\sqrt{a}, 0, 0)$ contained in the ellipses E_{xz} and E_{xy}, supposed parameterized in the neighborhood of p_0 by arc length with unitary tangent vector X_1 and X_2 respectively.

Also consider the orientation of the ellipsoid such that $k_1(p_0) > k_2(p_0) > 0$.

The principal curvatures of the ellipsoid on the coordinate planes are the curvature of the ellipses and as $a > b > c > 0$ it follows that $X_2(X_2(k_2))(p_0) < 0$.

Therefore $\xi_2(\theta_2)(p_0) = X_2(X_2(k_2))(k_2 - k_1)(p_0) > 0$ and, using Theorem 13, we see that this point is a ridge beak-to-beak for $\mathcal{F}_{\frac{\pi}{2}}$.

As $a > b > c > 0$ the point $p_1 = (0, 0, \sqrt{c})$ contained in the ellipses E_{xz} and E_{yz}, ridge of $\mathcal{F}_0$, it follows that $0 < k_2(p_1) < k_1(p_1)$, $X_1(X_1(k_1))(p_1) > 0$ and $\xi_1(\theta_1)(p_1) = X_1(X_1(k_1))(k_1 - k_2)(p_1) > 0$ and, using again Theorem 13, we see that this point p_1 is a ridge beak-to-beak for $\mathcal{F}_0$.

Therefore Theorem 13 implies that the ellipse E_{xz} is beak-to-beak for both principal curvatures.

Now consider the point $q_0 = (0, \sqrt{b}, 0)$ contained in the ellipse E_{yz} (ridge of k_2 corresponding to $\mathcal{F}_{\frac{\pi}{2}}$).

It follows that $k_1(q_0) > k_2(q_0) > 0$, $X_2(k_2)(q_0) = 0$ and $X_2(X_2(k_2))(p_0) > 0$.

Therefore $\xi_2(\theta_2)(q_0) = X_2(X_2(k_2))(k_1 - k_2)(q_0) < 0$ and the ellipse E_{yz} is zig-zag.

A similar argument shows that E_{xy} is zig-zag for k_1, i.e.,

$$X_1(X_1(k_1))(k_1 - k_2) < 0.$$

b) Hyperboloid of one sheet $(a > b > 0 > c)$

Consider the ellipse E_{xy} and an orientation of the hyperboloid such that $k_1 > 0 > k_2$ and k_1 being the curvature of this ellipse. For $p_0 = (\sqrt{a}, 0, 0) \in E_{xy}$, as $k_2 < 0$ it follows that $X_2(X_2(k_2))(p_0) > 0$ since the plane $z = 0$ is the plane of symmetry of the hyperbolas orthogonal to E_{xy}. Therefore $X_2(X_2(k_2))(p_0)(k_2 - k1)(p_0) < 0$ and E_{xy} is zig-zag for $\mathcal{F}_{\frac{\pi}{2}}$.

The hyperbola H_{yz} contained in the plane $x = 0$ is beak-to-beak for $\mathcal{F}_0$. In fact, let $q_0 = (0, \sqrt{b}, 0)$. So $X_1(X_1(k_1))(q_0) > 0$ (minimum of k_1 as $a > b$) and $X_1(X_1(k_1))(q_0)(k_1 - k_2)(q_0) > 0$. Analogously, it can be shown that H_{xz} is zig-zag for $\mathcal{F}_0$.

c) Hyperboloid of two sheets ($a > 0 > b > c$)

The analysis is similar to the case of the ellipsoid. □

4 Darboux curves on general cylinders, cones and surfaces of revolution

The Darboux curves on general cones were already studied by Santaló ([30]). In a similar way, one can study Darboux curves on cylinders and surfaces of revolution. This is not a coincidence. The three types of surfaces are canals corresponding to a curve $\gamma \subset \Lambda^4$ which is also contained in a 3-dimensional subspace of $\mathbb{R}^5_1$. Depending on the subspace, this intersection is either a copy of Λ^2, a unit sphere $\mathbb{S}^2$ or a 2-dimensional cylinder (see [2], [7], [24]). The latter condition defines conformal images of general cones, general cylinders and surfaces of revolution. These surfaces can be obtained imposing conformally invariant local conditions.

Recall first that canal surfaces are characterized locally, [2], [7], [17], [24], by the following proposition

Proposition 16. *A surface M is (a piece of) a canal if and only if one of its conformal principal curvatures, say θ_2, is equal to zero.*

Since Dupin cyclides are the only surfaces which are canal in two different ways, they can be characterized by the condition $\theta_1 = \theta_2 = 0$.

Proposition 17. *A surface such that $\theta_2 = 0$ and θ_1 is constant along characteristic circles can be obtained as the image by a Möbius map of a cone, a cylinder or a surface of revolution.*

The authors of [2] call the surfaces characterized in Proposition 17 *special canal surfaces*. Theorem 9 implies the following corollary.

Corollary 18. *The Darboux plane-field $\mathcal{D}$ is integrable when the surface M is a special canal.*

Proposition 19. *Let M be a special canal surface and (u, v) be a principal chart such that $\theta_1(u, v) = \theta_1(u)$ and $\theta_2(u, v) = 0$. As usual, E, F and G are the coefficients of the first fundamental form of M (here $F = 0$).*

Let $A(u) = \exp[\int \frac{k_1'}{k_1 - k_2} du]$ and $\alpha \in (0, \pi)$ be an angle. Then the function $\mathcal{J}(u, \alpha) = A(u) \cos^3 \alpha$ is a first integral of the Darboux curves. Moreover in the region $A_c = \pi(M_c) = \{(u, v) : u \in M_c\}$, $M_c = \mathcal{J}^{-1}(c)$, the Darboux curves are defined by the implicit differential equation

$$c^{2/3} G dv^2 - E(A^{2/3} - c^{2/3}) du^2 = 0.$$

Proof. In order to integrate a vector field in dimension 3, it is usual to look for a foliation the leaves of which contains the orbits, or even better, a foliation given by the levels of a function called *first integral*. Here the integrability of the Darboux plane-field $\mathcal{D}$ in $V(M) \subset \Lambda^4$ defines a foliation of $V(M)$ which can be lifted to $T^1 M$. Therefore, when $\mathcal{D}$ is integrable it is natural to try to find a global first integral.

When the 3-dimensional space is the "phase space" $T^1(M)$, a first integral gives a differential equation of order 1 on each level.

The differential equation (6) reduces to

$$u' = \frac{\cos \alpha}{\sqrt{E}}, \quad v' = \frac{\sin \alpha}{\sqrt{G}}, \quad \alpha' = \frac{1}{3\sqrt{E}} \frac{k_1'}{k_1 - k_2} \frac{\cos^2 \alpha}{\sin \alpha}.$$

Therefore,

$$\frac{d\alpha}{du} = \frac{1}{3} \frac{k_1'}{k_1 - k_2} \frac{\cos \alpha}{\sin \alpha}$$

which is an equation where the variables are separable. Direct integration leads to the first integral $\mathcal{J}$ as stated.

To obtain the implicit differential equation solve the equation $\mathcal{J}(u, v) = c$ in function of $\cos \alpha$ and observe that

$$\frac{dv}{du} = \frac{\sqrt{E}}{\sqrt{G}} \frac{\sin \alpha}{\cos \alpha}.$$

□

4.1 Cylinders

The case of cylinders is the simplest. Let $C = \{c(u)\}$ be a plane curve of curvature $k(u)$. The cylinder of axis generated by a vector $\vec{z}$ orthogonal to the plane can be parametrized by $\phi(u, v) = c(u) + v\vec{z}$. The function $\mathcal{I}(u, \alpha) = k(u) \cos^3 \alpha$ is a first integral for Darboux curves.

4.2 Cones

Proposition 20. *The Darboux curves on a cone free of umbilical points (that is without flat points) can be integrated by quadrature. The function*

$$\mathcal{I}(u, \alpha) = k_g(u) \cos^3 \alpha$$

is a first integral of the differential equation of Darboux curves. Here k_g is the geodesic curvature of the intersection of the cone with the unitary sphere.

Moreover, if $k_g'/k_g < 0$ the ridge is zig-zag. If $k_g'/k_g > 0$ the ridge is beak-to-beak. See Figure 9.

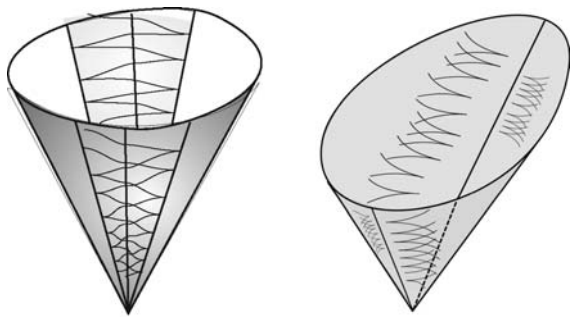

Figure 9: Darboux curves near regular ridges on a general cone.

Proof. The cone can be parametrized by $X(u, v) = v\gamma(u)$ where $|\gamma| = 1$ and $|\gamma'| = 1$ is a spherical curve.

Since $\gamma'' = -\gamma + k_g \gamma \wedge \gamma'$ and $N(u, v) = \gamma \wedge \gamma'$, $k_1(u, v) = k_g(u)$ and $k_2(u, v) = 0$.

Therefore, Darboux curves are given by $(\sin\alpha/\cos\alpha)d\alpha = \frac{1}{3}(k_g'/k_g)du$ and $\mathcal{I}(u, \alpha) = k_g(u)\cos^3\alpha$ is a first integral for them. The behavior of Darboux curves near ridges follows from Theorem 13. □

4.3 Surfaces of revolution

Traditionally, a surface of revolution is defined from a profile. Here we view it as a canal surface obtained from a one parameter family of spheres of radii $r(u)$ and centers at $(0, 0, u)$ on the vertical axis. The functions h, horizontal distance to the axis of revolution, r and β, angle between the tangent to the profile and the axis of revolution, are related by $h = r\cos\beta$.

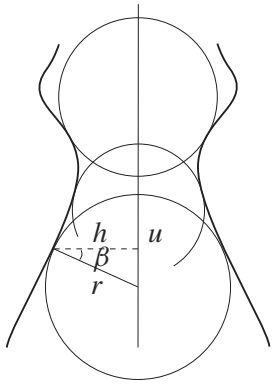

Figure 10: A surface of revolution as a canal.

The envelope of this family is a canal surface and can be parametrized by

$$H(u, v) = r(u)\cos\beta(u)(\cos v, \sin v, 0) + (0, 0, u - r(u)\sin\beta(u)),$$

where $\cos\beta(u) = \sqrt{1 - r'(u)^2}$, $\sin\beta = r'$, $|r'(u)| < 1$, $\beta \in (-\pi/2, \pi/2)$.

The unit normal to the surface is

$$N = (-\cos\beta(u)\cos v, -\cos\beta(u)\sin v, \sin\beta(u)).$$

The coefficients of the first and second fundamental forms of H are given by

$$E(u, v) = \frac{(1 - r'^2 - rr'')^2}{1 - r'^2}, \qquad F(u, v) = 0, \qquad G(u, v) = r^2(1 - r'^2)$$

$$e(u, v) = -\frac{r''(1 - r'^2 - rr'')}{1 - r'^2}, \qquad f(u, v) = 0, \qquad g(u, v) = r(1 - r'^2).$$

The principal curvatures are given by

$$k_1(u, v) = k_1(u) = -\frac{r''}{1 - r'^2 - rr''} \qquad k_2(u, v) = k_2(u) = \frac{1}{r}.$$

It will be assumed that the surface is free of umbilical points, for example that $k_2 > k_1$.

Therefore it follows that

$$\theta_1 = \frac{4r^2[r'''(1 - r'^2) + 3r'r''^2]}{(1 - r'^2)^{3/2}(1 - r'^2 - rr''))} = \frac{4r^2 R(u)}{(1 - r'^2)^{3/2}(1 - r'^2 - rr''))}, \qquad \theta_2 = 0.$$

Ridges corresponding to the principal foliation $\mathcal{F}_0$ are defined by the equation $\theta_1(u) = 0$ which is equivalent to

$$R(u) = \frac{\partial k_1}{\partial u} = r'''(1 - r'^2) + 3r'r''^2 = 0.$$

As $\theta_2 = 0$ the ridges corresponding to $\mathcal{F}_{\frac{\pi}{2}}$ is the whole surface of revolution.

Proposition 21. *The function*

$$\mathcal{I}(u, \alpha) = r(u)\cos\beta(u)(k_1 - k_2)\cos^3\alpha = h(u)(k_1 - k_2)\cos^3\alpha,$$

is a first integral of the differential equation of Darboux curves, where h is the distance of the point $H(u, v)$ of the surface to the axis of revolution.

Moreover, if $R'(u) < 0$, or equivalently $\xi_1(\theta_1) < 0$, the ridge is zig-zag. If $R'(u) > 0$, or equivalently, $\xi_1(\theta_1) > 0$ the ridge is beak-to-beak, see Figure 11, left beak-to-beak and right zig-zag.

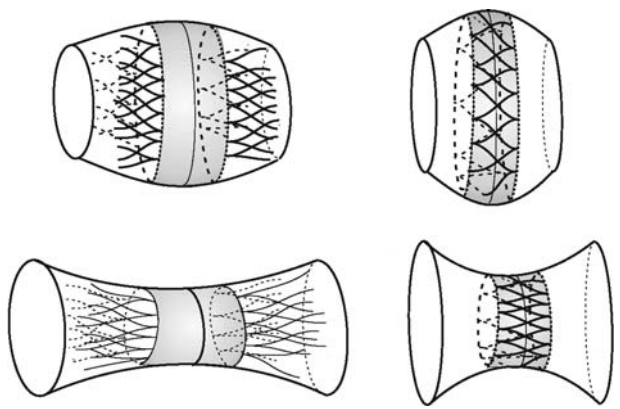

Figure 11: Darboux curves near regular ridges on surfaces of revolution, left beak-to-beak and right zig-zag.

Proof. In the principal chart (u, v) the differential equation of Darboux curves is given by

$$u' = \frac{1}{\sqrt{E}}\cos\alpha, \quad v' = \frac{1}{\sqrt{G}}\sin\alpha, \ \alpha' = \frac{1}{3\sqrt{E}}\left[\frac{k_1'(u)}{k_1(u) - k_2(u)}\right]\frac{\sin^2\alpha}{\cos\alpha}.$$

Therefore, it follows that $3\frac{\sin\alpha}{\cos\alpha}d\alpha = \frac{k_1'}{k_1 - k_2}du$.

Now observe that

$$\int \frac{k_1'}{k_1 - k_2} du = \int \frac{k_1' - k_2'}{k_1 - k_2} du + \int \frac{k_2'}{k_1 - k_2} du$$
$$= \ln(k_2 - k_1) + \int \frac{k_2'}{k_1 - k_2} du$$
$$\int \frac{k_2'}{k_1 - k_2} du = \int \left[\frac{r'}{r} + \frac{r' r''}{1 - r'^2} \right] du = \ln r (1 - r'^2)^{1/2}$$

Therefore

$$\mathcal{I}(u, v, \alpha) = r(1 - r'^2)^{1/2} (k_1 - k_2) \cos^3 \alpha$$
$$= r \cos \beta (k_1 - k_2) \cos^3 \alpha = h(u)(k_1 - k_2) \cos^3 \alpha$$

is the first integral. Again, the behavior of Darboux curves near ridges follows from Theorem 13. □

First notice that the osculating spheres of curvature k_1 of the surface of revolution intersect a plane containing the axis of revolution in the osculating circles of the profile. They form a surface $\mathcal{O}_1 \subset \Lambda^4$ (see 2). The osculating spheres of radius k_2 intersect the same plane in the circle of center $(0, u)$ and radius $r(u)$. They form a curve $\gamma \subset \Lambda^2 \subset \Lambda^4$.

Ridges on a surface of revolution are characteristic circles. They correspond to vertices of the profile. They also correspond to the singularities of the surface $\mathcal{O}_1 \subset \Lambda^4$ (see Figure 2).

Here the osculating spheres to the surface along a meridian form a curve C_{me} in a totally geodesic $\Lambda^2 \subset \Lambda^4$. We can also see this curve as corresponding to the osculating circles of the profile. The vertices of the profile correspond to singular points of C_{me}. At these singular points the tangent direction is light-like. The one-parameter family of rotations g_t leaving the surface of revolution invariant extend to a one-parameter family of isometries of the Lorentz space $\mathbb{R}^4_1$ such that $\mathcal{O}_1 = \cup g_t(C_{me})$.

5 Darboux curves on quadrics

The Darboux curves in the ellipsoid were considered by A. Pell in [25] and J. Hardy in [16]. Here we complete and hopefully simplify these works, describing the global behavior of Darboux curves in a triple orthogonal system of quadrics.

A geometrical aspect of the theory of quadrics is the following classical result. Given three straight lines L_1, L_2 and L_3 in $\mathbb{E}^3$ in general position the set of lines

intersecting these lines defines a one parameter family of lines which generate a unique twice ruled surface. This was first established by G. Monge [23]. See also Spivak [32]. The basic idea is observe that this configuration is of projective nature and also can be extended to the projective space $\mathbb{P}^3$. Taking coordinates such that the lines L_i are parallel to the axis and writing the equation of a general line L as the intersection of two planes $y = ax + b,\ z = cx + d$ it follows, from algebraic manipulations, that the set of lines which intercept the three given lines is a quadric, the hyperboloid of one sheet or the hyperbolic paraboloid.

A circle (or a line) contained in a surface is a Darboux curve. In fact, we can chose a sphere tangent to the surface in the pencil of spheres containing the circle or the line. The corresponding curve in Λ^4 is a geodesic, therefore it is a geodesic in $V(M)$, proving that the initial curve is a Darboux curve.

The quadratic surfaces have many remarkable geometric properties. Some were already considered by d'Alembert [1], who was the first to observe that the ellipsoid has two families of circular sections. After that, Monge and Hachette [23] showed that all generic quadric surfaces have two families of circular sections. Therefore, the 3-dimensional set $V(Q)$ of spheres having a saddle tangency with the quadric Q contains a surface filled with two families of geodesics, arcs of the pencils of spheres containing the previous circles. The previous analysis of twice rules surfaces in $\mathbb{P}^3$ shows that the latter surface is a piece of the intersection of Λ^4 with a quadratic cone of $\mathbb{R}^5_1$ contained in some hyperplane (see also [10]).

Recall that the a non singular quadric $\mathbb{Q}_{a,b,c}$ belongs to the triple orthogonal system of quadrics of equation $q(\lambda) = 0$ where

$$q(\lambda) = \frac{x^2}{a-\lambda} + \frac{y^2}{b-\lambda} + \frac{z^2}{c-\lambda} - 1$$

(we supposed $abc \neq 0$ and that $a > b > c > 0$; the other cases can be treated similarly; see also [32], vol. 3, chapter 4 and [33], pp. 99 to 103).

Given a point $p_0 = (x_0, y_0, z_0) \in \mathbb{Q}_{a,b,c}$ with $x_0 y_0 z_0 \neq 0$ the equation $q(\lambda) = 0$ is a polynomial of degree 3 in λ which has three real roots $\lambda_1 = 0$, $\lambda_2(p_0) \in]b, c[$ and $\lambda_3(p_0) \in]b, a[$. In fact the rational function $q(\lambda)$ has the same roots and poles at a, b and c. This forces one root in each of the intervals $]c, b[$ and $]b, a[$.

The position of the roots $\lambda_2 \in]c, b[$ and $\lambda_3 \in]b, a[$ implies that $q(\lambda_2(p_0)) = 0$ is an hyperboloid of one sheet and $q(\lambda_3(p_0)) = 0$ is an hyperboloid of two sheets. Moreover the surfaces $q(\lambda_2(p_0)) = 0$, $q(\lambda_3(p_0)) = 0$ and $q(0) = 0$ intersect orthogonally along the curves of intersections, see [33] [pp. 99 to 103]]). Dupin's theorem shows that these are lines of principal curvature, therefore the

curves $q(\lambda_2(p_0)) = q(0) = 0$ and $q(\lambda_3(p_0)) = q(0) = 0$ are the lines of principal curvature of the ellipsoid $\mathbb{Q}_{a,b,c}$ through the point p_0.

Consider the principal chart (u, v) and the parameterization β of $\mathbb{Q}_{a,b,c}$ given by equation (9) below.

$$\beta(u, v) = \left(\sqrt{\frac{a(u-a)(v-a)}{(b-a)(c-a)}},\ \sqrt{\frac{b(u-b)(v-b)}{(b-a)(b-c)}},\ \sqrt{\frac{c(u-c)(v-c)}{(c-a)(c-b)}} \right). \quad (9)$$

The first fundamental form of β is given by

$$I = ds^2 = Edu^2 + Gdv^2 = \frac{(v-u)u}{4H(u)}du^2 + \frac{(u-v)v}{4H(v)}dv^2 \quad (10)$$

The second fundamental form of β with respect to the normal $N = -(\beta_u \wedge \beta_v)/\|\beta_u \wedge \beta_v\|$ is given by

$$II = edu^2 + gdv^2 = \frac{(v-u)}{4H(u)}\sqrt{\frac{abc}{uv}}du^2 + \frac{(u-v)}{4H(v)}\sqrt{\frac{abc}{uv}}dv^2 \quad (11)$$

where $H(t) = (t-a)(t-b)(t-c)$.

Therefore the principal curvatures $k_1 \geq k_2$ are given by

$$k_1 = \frac{e}{E} = \frac{1}{u}\sqrt{\frac{abc}{uv}}, \qquad k_2 = \frac{g}{G} = \frac{1}{v}\sqrt{\frac{abc}{uv}}. \quad (12)$$

The four umbilics U_i, $(i = 1, \ldots, 4)$, are given by

$$(x_0, 0, z_0) = \left(\sqrt{\frac{a(a-b)}{a-c}},\ 0,\ \sqrt{\frac{c(c-b)}{c-a}} \right). \quad (13)$$

Recall that the domains of the principal charts (u, v) in the family of triply orthogonal systems of surfaces have the following restrictions:

- For the ellipsoid, with $a > b > c > 0$, $u \in (b, a)$, $v \in (c, b)$ or $u \in (c, b)$, $v \in (b, a)$.
- For the hyperboloid of one sheet, with $a > b > 0 > c$, $u \in (b, a)$, $v < c$ or $u < c$, $v \in (b, a)$.
- For the hyperboloid of two sheets, with $a > 0 > b > c$, $u \in (c, b)$, $v < c$ or $u < c$, $v \in (c, b)$. See Figure 12

See Figure 13 for an illustration of the region $x > 0$, $y > 0$, $z > 0$ of the ellipsoid parametrized by $\beta : [b, a] \times [c, b] \to \mathbb{Q}_{a,b,c}$, see (9), with the vertex (b, b) mapped to the umbilic $(x_0, 0, z_0)$, $\beta(b, c) = (a, 0, 0)$, $\beta(a, c) = (0, b, 0)$ and $\beta(a, b) = (0, 0, c)$.

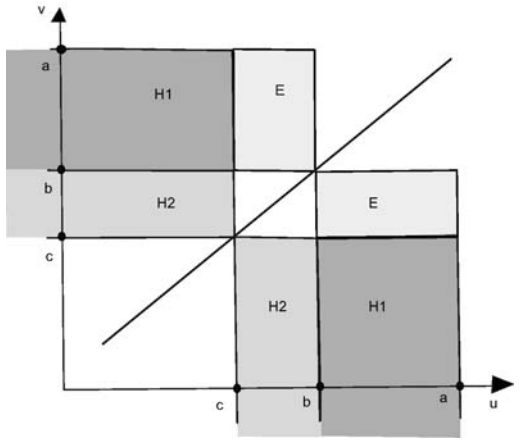

Figure 12: Domain of parametrization by a principal chart (u, v).

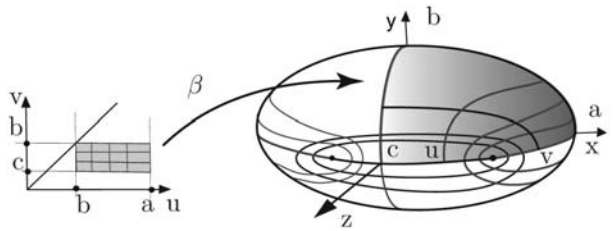

Figure 13: Parametrization of the ellipsoid by a principal chart (u, v).

5.1 Integrability of the Darboux plane-field on quadrics

Before studying the dynamics of Darboux curves on quadrics, let us prove the following

Proposition 22. *The Darboux plane-fields $\mathcal{D}$ of quadrics are integrable.*

Proof. Consider again the quadric $\mathbb{Q}_{a,b,c}$ defined by $\frac{x^2}{a} + \frac{y^2}{b} + \frac{z^2}{c} = 1$ with $a > b > c$, $abc \neq 0$, and let (u, v) a principal chart defined by Equation (9). Using the criterium of integrability given in Corollary 10, Equation 8, the result follows by elementary calculations using the formulas

$$k_1(u, v) = \frac{1}{u}\sqrt{\frac{abc}{uv}}, \quad k_2(u, v) = \frac{1}{v}\sqrt{\frac{abc}{uv}}$$

(Equation 12), giving the two principal curvatures of quadrics in the principal chart (u, v). □

The integrability of $\mathcal{D}$ guarantees the existence of a local first integral of the field $\mathcal{D}_1$, defined by

$$\begin{aligned}\mathcal{D}_1 &= \frac{\cos\alpha}{\sqrt{E}}\frac{\partial}{\partial u} + \frac{\sin\alpha}{\sqrt{G}}\frac{\partial}{\partial v} \\ &+ \left[\frac{\partial k_1/\partial u}{3\sqrt{E}(k_1-k_2)}\frac{\cos^2\alpha}{\sin\alpha} + \frac{\partial k_2/\partial v}{3\sqrt{G}(k_1-k_2)}\frac{\sin^2\alpha}{\cos\alpha}\right]\frac{\partial}{\partial\alpha}.\end{aligned} \tag{14}$$

Further forward we will provide a global one which allows us to achieve a qualitative analysis of Darboux curves on the quadrics $\mathbb{Q}_{a,b,c}$.

Proposition 23. *Consider the quadric $\mathbb{Q}_{a,b,c}$ and let (u, v) be a principal chart defined by equation* (9)*.*

Then the differential equation of Darboux curves on $\mathbb{Q}_{a,b,c}$ is given by

$$\begin{aligned}&u' = \frac{1}{\sqrt{E}}\cos^2\alpha\sin\alpha, \quad v' = \frac{1}{\sqrt{G}}\cos\alpha\sin^2\alpha \\ &\alpha' = r_1\cos^3\alpha + r_2\sin^3\alpha\end{aligned} \tag{15}$$

Here,

$$\begin{aligned}r_1 &= \frac{(k_1-k_2)\theta_1}{12} = \frac{1}{2}\frac{v}{u(u-v)}, \\ r_2 &= \frac{(k_1-k_2)\theta_2}{12} = \frac{1}{2}\frac{u}{v(u-v)} \\ E &= \frac{(v-u)u}{4H(u)} = \frac{(v-u)u}{4(u-a)(u-b)(u-c)}, \\ G &= \frac{(u-v)v}{4H(v)} = \frac{(u-v)v}{4(v-a)(v-b)(v-c)}.\end{aligned}$$

and α is the angle of the Darboux curve with the principal foliation $\mathcal{F}_0$. The differentiation is with respect to arc-length parametrization of the Darboux curve.

Proof. We can suppose that the Darboux curve is parametrized by arc-length (for the metric of the quadric $\mathbb{Q}_{a,b,c}$); then the vector $(\sqrt{E}u', \sqrt{G}v')$ is unitary. The angle α between the Darboux curve and the foliation $\mathcal{F}_0$ satisfies

$$\tan\alpha = \frac{\sqrt{G}v'}{\sqrt{E}u'} \quad \text{so that} \quad u' = \frac{1}{\sqrt{E}}\cos\alpha \quad \text{and} \quad v' = \frac{1}{\sqrt{G}}\sin\alpha.$$

In a principal chart the differential equation of Darboux curves is given by equation (6). Therefore, we have that

$$\begin{aligned} u' &= \frac{1}{\sqrt{E}}\cos\alpha \qquad v' = \frac{1}{\sqrt{G}}\sin\alpha \\ \frac{d\alpha}{ds_c} &= \frac{2}{k_1 - k_2}\frac{d\alpha}{ds} = \frac{1}{6\sin\alpha\cos\alpha}[\theta_1\cos^3\alpha + \theta_2\sin^2\alpha] \end{aligned} \tag{16}$$

To obtain a smooth vector field with the same orbits we multiply the vector-field given by Equation (16) by $\cos\alpha\sin\alpha(u', v', \alpha')$.

The coefficients r_1 and r_2 are obtained from the definition of θ_1 and θ_2, see Equation (3), and the values of E, F, k_1 and k_2, see Equations (10) and (12), in the principal chart (u, v) of the quadric. □

As the Darboux plane-field of quadrics is integrable (see Proposition 22), it is natural to look for a first integral for the vector field $\mathcal{D}_1$ defined by Equation (15) in the principal chart (u, v).

Proposition 24. *The function $I(u, v, \alpha) = k_n(\beta(u, v), \alpha)/\delta(\beta(u, v))$, where $k_n(\beta(u, v), \alpha)$ is the normal curvature in the direction making the angle α with $\mathcal{F}_0$ at $\beta(u, v)$ and δ is the distance of the tangent plane of the quadric at $\beta(u, v)$ to the origin of $\mathbb{E}^3$, is a first integral of* (15)*. In a principal chart (u, v) defined by equation* (9) *the first integral I writes*

$$I(u, v, \alpha) = \frac{\cos^2\alpha}{u} + \frac{\sin^2\alpha}{v}; \quad \tan\alpha = \frac{\sqrt{G}v'}{\sqrt{E}u'}. \tag{17}$$

Proof. Consider a principal chart (u, v) and the parametrization β defined by Equation (9).

The normal curvature in the direction ℓ defined by the unitary vector field

$$\left(\frac{u'}{\sqrt{E}}, \frac{v'}{\sqrt{G}}\right) = (\cos\alpha, \sin\alpha)$$

is given by

$$k_n(u, v, \alpha) = k_1(u, v)\cos^2\alpha + k_2(u, v)\sin^2\alpha = \sqrt{\frac{abc}{uv}}\left(\frac{\cos^2\alpha}{u} + \frac{\sin^2\alpha}{v}\right).$$

The distance of the tangent plane to the origin is given by

$$\delta(u, v) = \left\langle \frac{\beta_u \wedge \beta_v}{|\beta_u \wedge \beta_v|},\ \beta(u, v)\right\rangle = \sqrt{\frac{abc}{uv}}.$$

Then, $I(u, v, \alpha) = k_n(u, v, \alpha)/\delta(u, v) = \frac{\cos^2\alpha}{u} + \frac{\sin^2\alpha}{v}$.

Let $c(s) = (u(s), v(s), \alpha(s))$ be a solution of the differential equation (15). Let us show that $\frac{d}{ds}(I(u(s), v(s), \alpha(s)) = 0$.

We have

$$E_s = \frac{1}{4}\frac{uv'}{H(u)} - \frac{1}{4}\frac{u'}{H(u)^2}[(u-2v)H(u) + (uv-u^2)H'(u)]$$

$$G_s = \frac{1}{4}\frac{vu'}{H(v)} - \frac{1}{4}\frac{v'}{H(v)^2}[(u-2v)H(v) + (v^2-uv)H'(v)]$$

Straightforward calculation leads to $\frac{d}{ds}(I(u(s), v(s), \alpha(s))) = 0$. □

Let us now give a geometrical interpretation of the differential equation of Equation (17) obtained from the first integral of Proposition 24.

Proposition 25. *The Darboux curves on the quadric $\mathbb{Q}_{a,b,c}$ are the integral curves of the one parameter family (η being the parameter) of implicit differential equations*

$$k_n(\beta(u, v), \alpha) = \frac{e(u, v)du^2 + g(u, v)dv^2}{E(u, v)du^2 + G(u, v)dv^2} = \frac{1}{\eta}\sqrt{\frac{abc}{uv}} = \frac{1}{\eta}(abc)^{1/4}\,\mathcal{K}^{1/4}.$$

where $\mathcal{K} = k_1k_2$ is the Gauss curvature of the quadric.

Proof. By Proposition 24 the Darboux curves are defined by the one parameter family of implicit differential equations $I = 1/\eta$ (levels of the first integral), which are equivalent to

$$\left(\frac{dv}{du}\right)^2 = \frac{(u-\eta)}{(v-\eta)}\frac{vE(u, v)}{uG(u, v)} = \frac{(u-\eta)H(v)}{(v-\eta)H(u)}.$$

This equation writes

$$(v-\eta)H(u)v'^2 - (u-\eta)H(v)u'^2 = 0,\ \ H(x) = (x-a)(x-b)(x-c). \quad (18)$$

As $k_n(\beta(u, v), \alpha) = \dfrac{e + g(dv/du)^2}{E + G(dv/du)^2}$, it follows from Equation (18) and from Equations (10) and (11) that $k_n(\beta(u, v), \alpha) = \dfrac{1}{\eta}\sqrt{\dfrac{abc}{uv}} = \frac{1}{\eta}(abc)^{1/4}\,\mathcal{K}^{1/4}$. This ends the proof. □

5.2 Darboux curves on ellipsoids

Proposition 26. *Consider the ellipsoid $\mathbb{Q}_{a,b,c}$ with $a > b > c > 0$.*

i) *For $c < \eta < b$ the Darboux curves are and contained in cylindrical region $c < v < \eta$ and the behavior is as in Figure 14, upper left.*

ii) *For $\eta = b$ the Darboux curves are the circular sections of the ellipsoid. These circles are contained in planes parallels to the tangent plane to $\mathbb{Q}_{a,b,c}$ at the umbilical points. These circles are tangent along the ellipse E_y and through each umbilical point only one Darboux curve passes. See Figure 14, bottom right.*

iii) *For $b < \eta < a$ the Darboux curves are bounded contained in the two cylindrical region $\eta \leq u \leq a$ and the behavior is as shown in the Figure 14, upper right.*

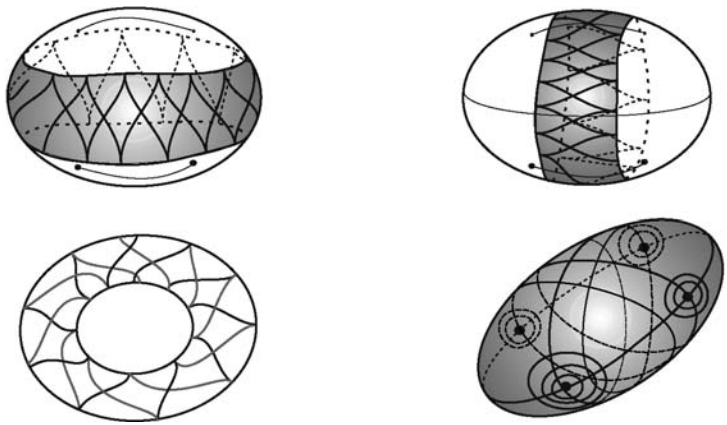

Figure 14: Darboux curves on the ellipsoid.

Proof. First case: $c < \eta < b$.

The differential equation of Darboux curves is given by:

$$\frac{(v-\eta)}{H(v)}v'^2 - \frac{(u-\eta)}{H(u)}u'^2 = 0, \quad c \leq v \leq \eta \quad \text{and} \quad b \leq u \leq a.$$

Define $d\tau_1 = \sqrt{(u-\eta)/H(u)}du$ and $d\tau_2 = \sqrt{(v-\eta)/H(v)}dv$.

Therefore the differential equation is equivalent to $d\tau_1^2 - d\tau_2^2 = 0$, with $(\tau_1, \tau_2) \in [0, L_1] \times [0, L_2]$ ($L_1 = \int_b^a d\tau_1 < \infty$, $L_2 = \int_c^\eta d\tau_2 < \infty$).

In the ellipsoid this analysis implies the following.

The cylindrical region $C_\eta = \alpha([b, a] \times [c, \eta])$ is foliated by the integral curves of an implicit differential equation having cusp singularities in ∂C_η. We observe that this region is free of umbilical point and is bounded by principal curvature lines, in coordinates defined by $v = c$ and $v = \eta$.

The case $b < \eta < a$ the analysis is similar. Now the differential equation of Darboux curves are defined in the region $[\eta, a] \times [c, b]$ and we have a cylindrical region $C_\eta = \alpha([\eta, a] \times [c, b])$.

For $\eta = b$ the differential equation can be simplified in the following

$$(u - a)(u - c)dv^2 - (v - a)(v - c)du^2 = 0.$$

This equation is well defined in the rectangle $[c, a] \times [c, a]$ which contains the $[b, a] \times [c, b]$.

Define $d\tau_1 = 1/\sqrt{(u - a)(u - c)}du$ and $d\tau_2 = 1/\sqrt{(v - a)(v - c)}dv$. So the equation is equivalent $d\tau_1^2 - d\tau_2^2 = 0$ with $(\tau_1, \tau_2) \in [0, L] \times [0, L]$ ($L = \int_c^a d\tau_1$). So in this rectangle all solutions are straight lines. The images of this family of curves on the ellipsoid are its circular sections. In fact we know that the ellipsoid has circular sections parallel to the tangent planes at umbilical points. As the circles are always Darboux curves it follows that the solutions of the differential equation is the family of circular sections. So we have two families of circles having tangency along the ellipse E_y. □

Remark. In Figure 14, a circle through an umbilic passes through the antipodal umbilical point only when $b^2 = (a^2 + c^2)/2$.

Proposition 27. *Consider an ellipsoid $\mathbb{Q}_{a,b,c}$ with three axes $a > b > c > 0$ and suppose $b < \eta < a$. Let $L_1 := \int_b^a \sqrt{E(u, b)}du$ and $L_2 := \int_c^\eta \sqrt{G(b, \eta)}du$ and define $\rho = \frac{L_2}{L_1}$. Consider the Poincaré map $\pi : \Sigma \to \Sigma$ associated to the foliation of Darboux curves defined by the implicit differential equation $I = 1/\eta$.*

Then if $\rho \in \mathbb{R} \setminus \mathbb{Q}$ (resp. $\rho \in \mathbb{Q}$) all orbits are recurrent (resp. periodic) on the cylinder region $v \leq \eta\}$. See Figure 14, bottom left.

Proof. The differential equation of Darboux curves is given by

$$\frac{(v - \eta)}{H(v)}v'^2 - \frac{(u - \eta)}{H(u)}u'^2 = 0, \quad c \leq v < \eta < u \leq a.$$

Define $d\tau_1 = \sqrt{\frac{(u-\eta)}{H(u)}}du$ and $d\tau_2 = \sqrt{\frac{(v-\eta)}{H(v)}}dv$. By integration, this leads to the chart (τ_1, τ_2), in a rectangle $[0, L_1] \times [0, L_2]$ in which the differential equation

of Darboux is given by

$$d\tau_1^2 - d\tau_2^2 = 0.$$

The result follows from the rotation number theory of circle diffeomorphisms, see [22] and [12]. □

5.3 Darboux curves on hyperboloids

Proposition 28. *Consider a connected component of a hyperboloid of two sheets $\mathbb{Q}_{a,b,c}$ with $a > 0 > b > c$.*

i) *For $\eta < c$ the Darboux curves are non bounded and contained in the non bounded region $v < \eta$ and the behavior is as in the Figure 15, left.*

ii) *For $\eta = c$ the Darboux curves are the circular sections of the hyperboloid. See Figure 15, center.*

iii) *For $c < \eta < b$ the Darboux curves are non bounded and contained in the cylindrical region $\eta \leq u \leq b$ and the local behavior is as shown in Figure 15, right.*

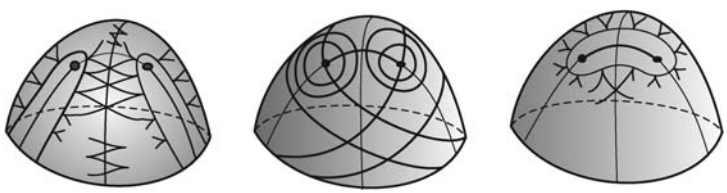

Figure 15: Darboux curves on a hyperboloid of two sheets.

Proof. The analysis developed in the case of the ellipsoid also works here. See proof of Proposition 26. □

Proposition 29. *Consider an hyperboloid of one sheet $\mathbb{Q}_{a,b,c}$ with $a > b > 0 > c$. Let $\eta \in (-\infty, c) \cup (b, \infty)$.*

i) *For $\eta < c$ the Darboux curves are bounded and contained in the cylindrical region $\eta \leq v \leq c$ and the behavior is as in Figure 16, upper center.*

ii) *For $b < \eta < a$ the Darboux curves are unbounded and contained in the cylindrical region $b \leq u \leq \eta$ (outside the hyperbola E_x) and the behavior is as in Figure 16, upper right.*

iii) *For $\eta = a$ the Darboux curves are the circular sections of the hyperboloid. See Figure 16, bottom left.*

iv) *For $a < \eta$ all Darboux curves are regular (helices) and go to ∞ in both directions. See Figure 16, bottom right.*

v) *The families of straight lines of the hyperboloid are not in the level sets of the first integral. See Figure 16, upper left.*

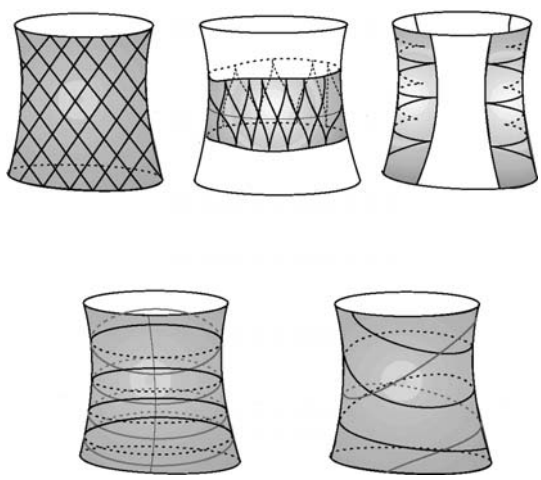

Figure 16: Darboux curves on a hyperboloid of one sheet.

Proof. Similar to the proof of Proposition 26. We observe that the hyperboloid of one sheet has two special families of Darboux curves, the straight lines and the circular sections. The family of circular sections are given by $\eta = a$ and that of straight lines are given by $\eta = \pm\infty$. □

Remark. We noticed in the analysis of Darboux curves that all quadrics have circular sections.

For instance, the circular sections of the hyperboloid

$$h(x, y, z) = \frac{x^2}{a^2} + \frac{y^2}{b^2} - \frac{z^2}{c^2} - 1 = 0$$

of one sheet are given by the intersection of the surface with the planes defined

by

$$\begin{aligned}\pi_1(y,z,u) &= \frac{\sqrt{a^2-b^2}}{b}y + \frac{\sqrt{a^2+c^2}}{c}z - u = 0\\ \pi_2(y,z,v) &= -\frac{\sqrt{a^2-b^2}}{b}y + \frac{\sqrt{a^2+c^2}}{c}z - v = 0\end{aligned} \tag{19}$$

where $u,\ v \in \mathbb{R}$.

In order to explain the result consider the intersection of $h^{-1}(0)$ with the sphere defined by $S(x, y, z) = x^2 + y^2 + z^2 - a^2 = 0$.

The key point here is that the sphere is bitangent to the hyperboloid at the points $(\pm a, 0, 0)$ with saddle contacts.

Elementary algebraic manipulations show that the intersection of these two surfaces are given by the intersections of the planes $\pi_i(y, z, 0)$ with the sphere $S(x, y, z) = 0$ and so are circular sections. To obtain the other circles, on needs to consider the bitangent spheres with two saddle contact point with the quadric.

A similar analysis can be done for the ellipsoid and hyperboloid of two sheets.

6 A few remarks and problems

Except on Dupin cyclides, most of the Darboux curves different from lines of principal curvature we encountered are not complete. Even the circles on quadrics are broken by singularities, as they have tangencies with the principal foliations.

Circles of homological type (1,1) on some cyclides surface spanned by two families of circles are examples of closed Darboux curve on a compact embedded surface. On smooth Dupin cyclides, there exist closed Darboux curves of any homology type (n, m). Notice that if two surfaces are tangent along a Darboux curve of one of them, this curve is also Darboux on the second surface. Therefore the examples above can be transfered on other surfaces.

We can also see that, given a generic curve in $\mathbb{E}^3$, it is possible to built a small ribbon containing the curve in its interior and such that the curve is a Darboux curve on the ribbon. We did not manage to construct such a ribbon when the curve has self accumulation points.

We do not know what is the local behavior of Darboux curves near Darbouxian umbilical points (see [13]).

On can generalize the notion of Darboux curves to higher dimensions. Let C be a curve contained in a hypersurface $M \subset \mathbb{E}^{n+1}$. Given an order of contact k, at each generic point m of a generic curve C, a k-osculating sphere Σ^k_m. When this sphere is always tangent to M, we say that the curve C is *k-Darboux*.

One could study the existence, geometry and dynamics of these curves.

Acknowledgements. The authors author are grateful to the faculty and staff of Institut de Mathématiques de Bourgogne (UMR CNRS **5584**), Université de Bourgogne-Franche-Comté, Instituto de Matemática e Estatística, Universidade Federal de Goiás and Wydział Matematyki i Informatyki Uniwersytetu Łódzkiego for the hospitality during there visits. The authors were supported by Pronex/FAPEG/CNPq Proc. 2012 10 26 7000 803, European Union (grant no. ICA1-CT-2002-70017/8), France-Brésil agreements 70017 and Polish National Science Center (grant no. 6065/B/HO3/2011/40).

References

[1] J. d'Alembert. *Opuscules mathémathiques ou Mémoires sur différens sujets de géométrie, de méchanique, d'optique, d'astronomie*. Tome VII, (1761), p. 163.

[2] A. Bartoszek, R. Langevin and P.G. Walczak. *Special canal surfaces of* $\mathbb{S}^3$. Bull. Braz. Math. Soc. New Series, **42**(2) (2011), 301–320.

[3] J.W. Bruce, P.J. Giblin and F. Tari. *Families of surfaces: focal sets, ridges and umbilics*. Math. Proc. Cambridge Philos. Soc., **125**(2) (1999), 243–268.

[4] R. Bryant. *A duality theorem for Willmore surfaces*. Journal of Differential Geometry, **20** (1984), 23–53.

[5] G. Cairns, R. Sharpe and L. Webb. *Conformal invariants for curves and surfaces in three dimensional space forms*. Rocky Mountain Jour. of Math., **24** (1994), 933–959.

[6] E. Cosserat. *Sur les courbes tracées sur une surface et dont la sphère osculatrice est tangente en chaque point à la surface*. Note Comptes Rendus Acad. Scien. Paris, **121** (1895), 43–46.

[7] G. Darboux. *Des courbes tracées sur une surface, dont la sphère osculatrice est tangente en chaque point à la surface*. Note Comptes Rendus Acad. Scien. Paris, tome LXXIII (1872), pp. 732–736.

[8] A. Enneper. *Bemerkungen über die Differentialgleichung einer Art von Curven auf Flächen*. Göttinger Nachrichten (1891), pp. 577–583.

[9] N. Fenichel. *Persistence and Smootheness of Invariant Manifolds of Flows*. Indiana University Math. J., **21** (1971-1972), 193–226.

[10] L.A. Florit. *Doubly ruled submanifolds in space forms.* Bull. Belg. Math. Soc. Simon Stevin, **13** (2006), 689–701.

[11] R. Garcia, R. Langevin and P. Walczak. *Darboux curves on surfaces I*, to appear in the Journal of the Mathematical Society of Japan.

[12] R. Garcia, R. Langevin and P. Walczak. *Foliations making a constant angle with principal directions on ellipsoids*. Ann. Polon. Math., **113** (2015), 165–173.

[13] R. Garcia and J. Sotomayor. *Differential Equations of Classical Geometry, a Qualitative Theory*. Publicações Matemáticas, 27° Colóquio Brasileiro de Matemática, IMPA, (2009).

[14] A. Gullstrand. *Zur Kenntniss der Kreispunkte*. Acta Math., **29** (1905), 59–100.

[15] J. Haantjes. *Conformal differential geometry.V. Special surfaces*. Nederl. Akad. Wetensch. Verslagen, Afd. Natuurkunde, **52** (1943), 322–331.

[16] J.G. Hardy. *Darboux lines on surfaces*. Amer. Journal of Mathematics, **20** (1898), 283–292.

[17] U. Hertrich-Jeromin. *Introduction to Möbius Differential Geometry*. London Math. Soc. Lecture Notes, vol. **300** Cambridge University Press (2003).

[18] M. Hirsh, C. Pugh and M. Shub. *Invariant Manifolds*. Lectures Notes in Math., **583** (1977).

[19] F. Klein. *Lectures on Mathematics*. Macmillan and company (1894), reprint AMS Chelsea publishing Providence, Rhode Island (2011 and 2000).

[20] R. Langevin and J. O'Hara. *Conformal arc-length as $\frac{1}{2}$ dimensional length of the set of osculating circles*. Comment. Math. Helvetici, **85** (2010), 273–312.

[21] R. Langevin and P.G. Walczak. *Conformal geometry of foliations*. Geom. Dedicata, **132** (2008), 135–178.

[22] W. Melo and J. Palis. *Geometric Theory of Dynamical Systems*. New York, Springer Verlag (1982).

[23] G. Monge et Hachette. *Application de l'analyse à la géométrie, Première Partie*, (1807), pp. 1–57.

[24] E. Musso and L. Nicoldi. *Willmore canal surfaces in Euclidean space*. Rend. Istit. Mat. Univ. Trieste, **31** (1999), 177–202.

[25] A. Pell. *D-lines on Quadrics*. Trans. Amer. Math. Soc. vol. **1** (1900), 315–322.

[26] I.R. Porteous. *Geometric Differentiation*. Cambridge Univ. Press (2001).

[27] M. Ribaucour. *Propriétés de courbes tracées sur les surfaces*. Note Comptes Rendus Acad. Scien. Paris, Tome LXXX, (1875), pp. 642–645.

[28] R. Roussarie. *Modèles locaux de champs et de formes*. Astérisque, **30** (1975), pp. 181.

[29] L.A. Santaló. *Curvas extremales de la torsion total y curvas-D*. Publ. Inst. Mat. Univ. Nac. Litoral. (1941), pp. 131–156.

[30] L.A. Santaló. *Curvas D sobre conos*. Select Works of L.A. Santaló, Springer Verlag (2009), pp. 317–325.

[31] F. Semin. *Darboux lines*. Rev. Fac. Sci. Univ. Istanbul (A), **17** (1952), 351–383.

[32] M. Spivak. *A Comprehensive Introduction to Differential Geometry*, vol. III, Publish of Perish Berkeley (1979).

[33] D. Struik. *Lectures on Classical Differential Geometry*. Addison Wesley (1950), Reprinted by Dover Collections (1988).

[34] M.A. Tresse. *Sur les invariants différentiels d'une surface par rapport aux transformations conformes de l'espace*. Note Comptes Rendus Acad. Sci. Paris, **192** (1892), 948–950.

[35] E. Vessiot. *Contributions à la géométrie conforme. Cercles et surfaces cerclées*. J. Math. Pures Appliqués, **2** (1923), 99–165.

Ronaldo Garcia
Instituto de Matemática e Estatística
Universidade Federal de Goiás
Caixa Postal 131
74001-970 Goiânia, GO
BRAZIL

E-mail: ragarcia@ufg.br

Rémi Langevin
Institut de Mathématiques de Bourgogne
UMR CNRS 5584, U.F.R. Sciences et Techniques
9, avenue Alain Savary
Université de Bourgogne-Franche-Comté, B.P. 47870
21078 – DIJON Cedex
FRANCE

E-mail: Remi.Langevin@u-bourgogne.fr

Paweł Walczak
Katedra Geometrii
Wydział Matematyki i Informatyki
Uniwersytet Łódzki
ul. Banacha 22, 90-238, Łódź
POLAND

E-mail: pawelwal@math.uni.lodz.pl